Numerical Analysis of Natural Convection in Porous Cavity with Partial Convective Cooling Condition

W. Pakdee[1] and P. Rattanadecho
Department of Mechanical Engineering, Faculty of Engineering,
Thammasat University, Rangsit Campus,
Klong Luang, Pathumtani 12120, Thailand
Tel: 011 662 5643001-5, Fax: 011 662 5643010

Abstract

The transient natural convection flow through a fluid-saturated porous medium in a square enclosure with a partially cooling surface condition was investigated using Brinkmann-extended Darcy model. Physical problem consists of a rectangular cavity filled with porous medium. The cavity is insulated except the top wall that is partially exposed to an outside ambient. The exposed surface allows convective transport through the porous medium, generating a thermal stratification and flow circulations. The formulation of differential equations is nondimensionalized and then solved numerically under appropriate initial and boundary conditions using the finite difference method. The finite difference equations handling the convection boundary condition of the open top surface are derived for cooling condition. In addition to the negative density gradient in the direction of gravitation, a lateral temperature gradient in the region close to the top wall induces the buoyancy force under an unstable condition. The two-dimensional flow is characterized mainly by the clockwise and anti-clockwise symmetrical vortices driven by the effect of buoyancy. The directions of vortex rotation generated under the cooling condition are in the opposite direction as compared to the heating condition. Unsteady effects of associated parameters were examined. The modified Nusselt number (Nu) is systematically derived. This newly developed form of Nu captures the heat transfer behaviors reasonably accurately. It was found that the heat transfer coefficient, Rayleigh number, Darcy number as well as flow direction strongly influenced characteristics of flow and heat transfer mechanisms.

Keywords: convective transport, numerical analysis, saturated porous media, convection boundary condition, partial cooling

[1] Author to whom correspondence should be addressed; E-mail address: pwatit@engr.tu.ac.th, and wpele95@yahoo.com

Nomenclature

c_p specific heat capacity [J/kgK]

Da Darcy number [-]

g gravitational constant [m/s^2]

H cavity length [m]

h convective heat transfer coefficient [W/m^{2}K]

k thermal conductivity of the porous medium [W/mK]

p pressure [Pa]

Pr Prandtl number [-]

Ra Rayleigh number [-]

T temperature [C]

t time [s]

u, v velocity component [m/s]

x, y Cartesian coordinates

X, Y dimensionless Cartesian coordinates

W cavity width [m]

Greek symbols

κ permeability of porous medium[m^2]

α thermal diffusivity [m^2/s]

β coefficient of thermal expansion [1/K]

ε porosity [-]

μ dynamic viscosity [Pa/s]

ν kinematics viscosity [m^2/s]

ρ_f fluid density [kg/m^3]

τ dimensionless time

θ dimensionless temperature

ω vorticity [s^{-1}]

ψ stream function [m^2/s]

ς dimensionless vorticity

Ψ dimensionless stream function

Subscripts

∞ ambient condition

i initial condition and index for a number of points in x direction

j index for a number of points in y-direction

e effective

1. Introduction

The convective heating or cooling that causes heat and fluid flows inside cavity is found in various applications including lakes and geothermal reservoirs, underground water flow, solar collector etc. (Bergman et al., 1986). Associated industrial applications include secondary and tertiary oil recovery, growth of crystals (Imberger and Hamblin, 1982), heating and drying process (Stanish et al., 1986; Rattanadecho et al., 2001, 2002), electronic device cooling, solidification of casting, sterilization etc. Natural or free convection in a porous medium has been studied extensively. Cheng (1978) provides a comprehensive review of the literature on free convection in fluid-saturated porous media with a focus on geothermal systems. In the framework of porous media models, Darcy proposed the phenomenological relation between the pressure drop across a saturated porous medium and the flow rate. The Darcy model has been employed in the recent investigations. Bradean et al. (1997) assumed Darcy's law and used Boussinesq approximation to numerically simulate the free convection flow in a porous media adjacent to vertical or horizontal flat surface. The surface is suddenly heated and cooled sinusoidally along its length. The Darcy law with the Boussinesq approximation was also employed by Bilgen and Mbaye (2001) to study the development of Be'n-ard cell in fluid-saturated porous cavity whose lateral walls are cooled. It was found that the existence of two convective solution branches is related to the Darcy-Rayleigh and Biot numbers. Recently, a numerical study was conducted to solve the problem of thermosolutal convection within a rectangular enclosure (Bera and Khalili, 2002). The results revealed that anisotropy causes significant changes in Nusselt and Sherwood numbers. Many works of flow in porous media, such as ones addressed above, have used the Darcy law. Although the Darcy law is applicable to slow flows, it does not account for initial and boundary effects. In the situation when the flow is strong, and solid boundary effect and viscous effect are not negligible, these effects termed non-Darcy effects, become important (Khanafer and Chamkha, 1998). Bera et al. (1998) considered double diffusive convection due to constant heating and cooling on the two vertical walls, based on a non-Darcy model inclined permeability tensor. Two distinguished modifications of Darcy' law are the Brinkmann's and the Forchheimer's extensions which treats the viscous stresses at the bounding walls and the non-linear drag effect due to the solid matrix respectively (Nithiarasu et al., 1997). The Darcy-Forchheimer- Brinkman model was used to represent the fluid transport within the porous medium in the investigation of a convective flow through a channel (Marafie and Vafai, 2001). In this work, the two-equation model was used to describe energy transport for solid and fluid phase. The Brinkman-extended Darcy model has been considered in a literature (Tong and Subramanian, 1985; Laurat and Prasad, 1987; Kim et al., 2001; Pakdee and Rattanadecho, 2006). Darcy-Forchheimer model has been used in a number of published works (Beckermann et al., 1985; Lauriat and Prasad, 1989; Basak et al., 2006). In the study of effects of various thermal boundary conditions applied to saturated porous cavity, the conduction dominant regime is within $Da \leq 10^{-5}$. Nithiarasu et al. (1998) examined effects of applied heat transfer coefficient on the cold wall of the cavity upon flow and heat transfer inside a porous medium. The differences between the Darcy and non-Darcy flow regime are clearly investigated for different Darcy, Rayleigh and Biot numbers and aspect ratio. Variations in Darcy, Rayleigh and Biot numbers and aspect ratio significantly affect natural flow convective pattern.

Natural convection flows with a variety of configurations were investigated for different aspects. Oosthuizen and Patrick (1995) performed numerical studies of natural convection in an inclined square enclosure with part of one wall heated to a uniform temperature and with the opposite wall uniformly cooled to a lower temperature and with the remaining wall portions. The enclosure is partially filled with a fluid and partly filled with a porous medium, which is saturated with the same fluid. The main results considered were the mean heat transfer rate across the enclosure. Nithiarasu et al. (1997) examined effects of variable porosity on convective flow patterns inside a porous cavity. The flow is triggered by sustaining a temperature gradient between isothermal lateral walls. The variation in porosity significantly affects natural flow convective pattern. Khanafer and Chamkha (1998) performed numerical study of mixed convection flow in a lid-driven cavity filled with a fluid-saturated porous media. In this study, the influences of the Richardson number, Darcy number and the Rayleigh number play an important role on mixed convection flow inside a square cavity filled with a fluid-saturated porous media. Recently, Al-Amiri (2000) performed numerical studies of momentum and energy transfer in a lid-driven cavity filled with a saturated porous medium. In this study, the force convection is induced by sliding the top constant-temperature wall. It was found that the increase in Darcy number induces flow activities causing an increase in the fraction of energy transport by means of convection. With similar description of the domain configuration, Khanafer and Vafai (2002) extended the investigation to mass transport in the medium. The buoyancy effects that create the flow are induced by both temperature and concentration gradients. It was concluded that the influences of the Darcy number, Lewis number and buoyancy ratio on thermal and flow behaviors were significant. Furthermore, the state of art regarding porous medium models has been summarized in the recently published books (Nield and Bejan, 1999; Vafai, 2000; Pop and Ingham, 2001; Basak et al., 2006).

Previous investigations have merely focused on momentum and energy transfer in cavity filled with a saturated porous medium subjected to prescribed temperature and prescribed wall heat flux conditions. However, only a very limited amount of numerical and experimental work on momentum and energy transfer in a cavity filled with a saturated porous medium subjected to heat transfer coefficient boundary condition at the exposed portion of the top wall has been reported. Moreover, only very few published work is pertinent to partially heated or cooled porous media although they are found in a number of applications such as in flush mounted electrical heater or buildings (Desai et al, 1997; Al-Amiri, 2002; Oztop, 2007). The very recent work of Oztop (2007) investigated natural convection in partially cooled and inclined porous enclosures. His study presented the steady state results within the enclosure of isothermal heated and cooled walls. In our study, the surface is partially cooled under the convective boundary condition, allowing the surface temperature to change with time. The convective cooling condition or so-called condition of the third kind is systematically derived. While the focus of the present study is on the cooling effect, our recently published work (Pakdee and Rattanadecho, 2006) studied the influence of partially heated surface on thermal/flow behaviors. In this previous work, although the results were qualitatively discussed in detail, no quantitative description of heat transfer in terms of Nusselt number (Nu) was reported. Therefore, in order to gain better insights into the analysis, our present study proposes a new formulation of Nu employed to analyze the heat transfer behaviors. Moreover, to the best knowledge of the authors, no attention has been paid to transient convection due to surface partial convective cooling.

In the present study, the quantitative study in terms of Nu is taken into account. The new formulation of Nu is developed to correctly capture heat transfer behaviors. The study of heat transfer due to cooling condition has been carried out for transient natural convective flow in a fluid-saturated porous medium filled in a square cavity. In contrast to the heating condition, the cooling condition changes the direction of the induced flows. The top surface is partially open to the ambient, allowing the surface temperature to vary, depending on the influence of convection heat transfer mechanism. Computed results are depicted using temperature, flow distributions and heat transfer rates in terms of local and average Nusselt numbers. The influences of associated parameters such as Rayleigh number and Darcy number on the flow and thermal configurations were examined.

2. Problem Description

The computational domain, depicted in figure. 1 is a rectangular cavity of size W×H filled with a fluid-saturated porous medium. Aspect ratio of unity (A=1) is used in the present study. The domain boundary is insulated except the top wall, which is partially exposed to an ambient air. The initial and boundary conditions corresponding to the problem are of the following forms.

$$u = v = 0,\ T = T_i \quad \text{for} \quad t = 0 \tag{1}$$

$$\left.\begin{aligned} u = v = 0 \quad & \text{at } x = 0, \mathrm{W} \quad 0 \le y \le \mathrm{H} \\ u = v = 0 \quad & \text{at } y = 0, \mathrm{H} \quad 0 \le x \le \mathrm{W} \end{aligned}\right\} \tag{2}$$

$$\left.\begin{aligned} \frac{\partial T}{\partial x} = 0 \quad & \text{at } x = 0, W \qquad 0 \le y \le \mathrm{H} \\ \frac{\partial T}{\partial y} = 0 \quad & \text{at } y = 0 \qquad\quad 0 \le x \le \mathrm{W} \\ \frac{\partial T}{\partial y} = 0 \quad & \text{at } y = H \quad 0 \le x \le \mathrm{L} \text{ and } \mathrm{W\text{-}L} \le x \le \mathrm{W} \end{aligned}\right\} \tag{3}$$

The boundary condition at the exposed portion of the top wall is defined as

$$-k\frac{\partial T}{\partial y} = \mathrm{h}[T - T_\infty] \quad \text{at } y = \mathrm{H} \qquad L \le x \le \mathrm{W\text{-}L}, \tag{4}$$

where k and h are effective thermal conductivity and convection heat transfer coefficient. This type of condition corresponds to the existence of convective heat transfer at the surface and is obtained from the surface energy balance.

The porous medium is assumed to be homogeneous and thermally isotropic. The saturated fluid within the medium is in a local thermodynamic equilibrium (LTE) with the solid matrix (El-Refaee et al., 1998; Nield and Bejan, 1999; Al-Amiri, 2002). The validity regime of local thermal equilibrium assumption has been established (Mohammad, 2000; Marafie and Vafai, 2001). The porous porosity is uniform. The fluid flow is unsteady, laminar and incompressible. The pressure work and viscous dissipation are all assumed negligible. The thermophysical properties of the porous medium are taken to be constant. However, the Boussinesq approximation takes into account of the effect of density variation on the buoyancy force, in which the fluid density is assumed constant except in the buoancy term of the equation of motion. Furthermore, the solid matrix is made of spherical particles, while the porosity and permeability of the medium are assumed to be uniform throughout the rectangular cavity. Using standard symbols, the governing equations describing the heat transfer phenomenon are given by

$$\frac{\partial u}{\partial x}+\frac{\partial v}{\partial y}=0 \tag{5}$$

$$\frac{1}{\varepsilon}\frac{\partial u}{\partial t}+\frac{u}{\varepsilon^2}\frac{\partial u}{\partial x}+\frac{v}{\varepsilon^2}\frac{\partial u}{\partial y}=-\frac{1}{\varepsilon\rho_f}\frac{\partial P}{\partial x}+\frac{\upsilon}{\varepsilon}\left(\frac{\partial^2 u}{\partial x^2}+\frac{\partial^2 u}{\partial y^2}\right)-\frac{\mu u}{\rho_f \kappa} \tag{6}$$

$$\frac{1}{\varepsilon}\frac{\partial v}{\partial t}+\frac{u}{\varepsilon^2}\frac{\partial v}{\partial x}+\frac{v}{\varepsilon^2}\frac{\partial v}{\partial y}=-\frac{1}{\varepsilon\rho_f}\frac{\partial P}{\partial y}+\frac{\upsilon}{\varepsilon}\left(\frac{\partial^2 v}{\partial x^2}+\frac{\partial^2 v}{\partial y^2}\right)+g\beta(T-T_\infty)-\frac{\mu v}{\rho_f \kappa} \tag{7}$$

$$\sigma\frac{\partial T}{\partial t}+u\frac{\partial T}{\partial x}+v\frac{\partial T}{\partial y}=\alpha\left(\frac{\partial^2 T}{\partial x^2}+\frac{\partial^2 T}{\partial y^2}\right) \tag{8}$$

$$\sigma=\frac{[\varepsilon(\rho c_p)_f+(1-\varepsilon)(\rho c_p)_s]}{(\rho c_p)_f}, \tag{9}$$

where κ is medium permeability, β is thermal expansion coefficient, α is effective thermal diffusivity of the porous medium, μ and υ are viscosity and kinematic viscosity of the fluid respectively. Symbols ε and ν denotes porosity of porous medium and fluid viscosity, respectively. In the present study, the heat capacity ratio σ is taken to be unity since the thermal properties of the solid matrix and the fluid are assumed identical (Bergman et al., 1986; Khanafer and Vafai, 2002). The momentum equation consists of the Brinkmann term, which describes viscous effects due to the presence of solid body (Brinkmann, 1947). This form of momentum equation is known as Brinkmann-extended Darcy model. Lauriat and Prasad (1987) employed the Brinkmann-extended Darcy formulation to investigate the buoyancy effects on natural convection in a vertical enclosure. Although the viscous boundary layer in the porous medium is very thin for most engineering applications, inclusion of this term is essential for heat transfer calculations (Al-Amiri, 2000). However, the inertial effect was neglected, as the natural convection flow was studied (Basak et al., 2006).

The variables are transformed into the dimensionless quantities defined as,

$$\left.\begin{aligned} &X=\frac{x}{H},\, Y=\frac{y}{H},\; \tau=\frac{t\alpha}{H^2},\; U=\frac{uH}{\alpha},\; V=\frac{vH}{\alpha} \\ &\varsigma=\frac{\omega H^2}{\alpha},\; \Psi=\frac{\psi}{\alpha},\; \theta=\frac{T-T_l}{T_h-T_l} \end{aligned}\right\}, \qquad (10)$$

where ω and ψ represent dimensional vorticity and stream function, respectively. Symbol α denotes thermal diffusivity. Temperatures T_l and T_h change their values according to the problem type. In the heating case, T_l is initial temperature of a medium, and T_h is an ambient temperature. In the other case of cooling, T_h is set to be an initial temperature of the medium, while T_l is an ambient temperature instead. The governing equations are transformed into a vorticity –stream function formulation. Thus the dimensionless form of the governing equations can be written as

$$\frac{\partial^2\Psi}{\partial X^2}+\frac{\partial^2\Psi}{\partial Y^2}=-\varsigma \qquad (11)$$

$$\varepsilon\frac{\partial\varsigma}{\partial\tau}+U\frac{\partial\varsigma}{\partial X}+V\frac{\partial\varsigma}{\partial Y}=\varepsilon\,\Pr\left(\frac{\partial^2\varsigma}{\partial X^2}+\frac{\partial^2\varsigma}{\partial Y^2}\right)+\varepsilon^2 Ra\Pr\left(\frac{\partial\theta}{\partial X}\right)-\frac{\varepsilon^2\Pr}{Da}\varsigma \qquad (12)$$

$$\sigma\frac{\partial\theta}{\partial\tau}+U\frac{\partial\theta}{\partial X}+V\frac{\partial\theta}{\partial Y}=\alpha\left(\frac{\partial^2\theta}{\partial X^2}+\frac{\partial^2\theta}{\partial Y^2}\right), \qquad (13)$$

$$U=\frac{\partial\Psi}{\partial Y},\quad V=-\frac{\partial\Psi}{\partial X} \qquad (14)$$

where the Darcy number, Da is defined as κ / H^2, and Pr= ν/α is Prandtl number, where α = $k_e/(\rho c_p)_f$ is the thermal diffusivity. The Rayleigh number Ra, which gives the relative magnitude of buoyancy and viscous forces, is defined as $Ra = g\beta(T_i - T_\infty)H^3/(\upsilon\alpha)$.

3. Numerical Procedure

The thermal properties of the porous medium are taken to be constant. Specific heat ratio of unity is assumed. The effective thermal conductivity of the porous medium considered is 10 W/m·K.

In the present study, the iterative finite difference method was used to solve the transient dimensionless governing equations (Eqs. (10)–(12)) subject to their corresponding initial and boundary conditions given by Eqs. (1)–(4). Central–difference formulae were used for all spatial derivatives. The transient transport equations, Eqs (12)–(13), were solved explicitly. Successive over relaxation method (SOR) was utilized to solve for the flow kinematics relation given by Eq. (11). The velocity components, *U* and *V*, were computed according to Eq. (14). Approximation of convective terms is based on a second–order upwind finite differencing scheme, which correctly represents the directional influence of a disturbance. A uniform grid resolution of 61 × 61 was found to be sufficient for all smooth computations and computational time required in achieving steady-state conditions. Finer grids did not provide a noticeable change in the computed results.

3.1 Convective cooling boundary condition

The finite difference form of boundary condition at the open part of the top surface is systematically derived, based on energy conservation principle. The boundary values of dimensionless temperature of a node i, j $\theta_{i,j}$ in the heating case are expressed as

$$\theta_{ij} = \frac{2\theta_{ij-1} + \theta_{i-1j} + \theta_{i+1j} + 2\dfrac{\text{h}\Delta y}{k}}{2(\dfrac{\text{h}}{k}\Delta Y + 2)}, \tag{15}$$

where ΔY is the mesh size in y-direction.

In the different case of cooling phenomenon, the expression is given by

$$\theta_{ij} = \frac{2\theta_{ij-1} + \theta_{i-1j} + \theta_{i+1j}}{2(\dfrac{\text{h}}{k}\Delta Y + 2)} \tag{16}$$

It can be noticed that both the equations (15) and (16) are independent of an ambient temperature T_∞ as it has been eliminated during the derivation. This feature is attractive since the solutions can be obtained regardless of a value of T_∞ .

3.1 Corrected formulation of Nusselt number

The local Nusselt number (Nu) at the cooled horizontal surface is used as a tool to determine the ratio of convection heat transfer to conduction heat transfer within the porous enclosure. The accurate derivation of Nu is extremely important from the standpoint of determining the rate of heat transfer occurring at a surface. Based on the concept of energy balance at the surface for the cooling case,

$$-k\left.\frac{dT}{dy}\right|_{y=H} = h(T_H - T_\infty), \tag{17}$$

where H is indicated in figure 1, and with the definition of Nu,

$$\text{Nu} = \frac{hH}{k} = -\frac{H}{(T_H - T_\infty)}\left.\frac{dT}{dy}\right|_{Y=H} \tag{18}$$

In terms of the dimensionless quantities θ and Y defined in the preceding equation (10), Nu will take the form,

$$\text{Nu} = -\frac{1}{\theta_H}\left.\frac{d\theta}{dY}\right|_{Y=1}, \tag{19}$$

where θ_H is the dimensionless temperature at the top surface.

The new formulation of Nu in the present work has not yet been found in the literature. This modified form of Nu takes into account of temperature variation at the cooled surface. The average Nusselt Number, $\overline{\mathrm{Nu}}$ is computed according to

$$\overline{\mathrm{Nu}} = \int_{L}^{W-L} \frac{\mathrm{Nu}(x)dx}{l}, \qquad (20)$$

where l is the length of the gap at the top wall.

In order to verify the accuracy of the present numerical study, the results obtained by the present numerical model were validated against the Benchmark solutions for natural convection in a cubic cavity (Wakashima and Saitoh, 2004). The comparisons tabulated in table 1 reveal an excellent agreement within 1.5 percent difference. Also present computed results were compared with those obtained by Aydin (2000) for a free convection flow in a cavity, with side-heated isothermal wall, filled with pure air (Pr = 0.7) for Rayleigh number of 10^4. It was found that the solutions have good agreement with the previously published work. The results of selected tests are given in table 2 that shows a good agreement of the maximum value of the stream function and the maximum values of the horizontal and vertical velocity components between the present solution and that of Aydin. Moreover, the results from the present numerical model were compared with the solution of Nithiarasu et al. (1997) in the presence of porous medium for additional source of confidence, as shown in figure 2 for streamlines and isotherms for which the compared contours have the same range of contour levels. The values of Ra = 10^4, Da = 0.01 and ε = 0.6 were chosen. Table 3 clearly shows a good agreement of the maximum values of the stream function and vertical velocity component between the present solution and that of Nithiarasu et al (1997). All of these favorable comparisons lend confidence in the accuracy of the present numerical model.

4. Results and Discussion

The following discussions include the numerical results from the present study, which focuses on transient flow and thermal behaviors. Initial values of θ for an entire domain are set 1, based on equation (10) as the ambient temperature is lower than temperature of the medium in cavity. The investigations were conducted for a range of controlling parameters, which are Darcy number (Da) Rayleigh number (Ra) and convective heat transfer coefficient (h). The uniform porosity ε of 0.8 and unity aspect ratio (A=1) were considered throughout in the present study. In order to assess global effects of these parameters, the streamlines and isotherm distributions inside the entire cavity are presented. All the figures have the same range of contour levels to facilitate direct comparisons.

The resulting computational fields were extracted at the time adequately long to ensure sufficient energy transferred throughout the domain. Figure 3 displays instantaneous images of the contour plots during the thermal and flow evolution. The Rayleigh number of 5×10^4, Da = 0.1, Pr = 1.0, h = 60 w/m^2K, and ε =0.8 are considered. The two columns represent contours of temperature and stream function respectively from left to right. With the same contour levels, comparisons can be made directly. The four snapshots from top to bottom in each column are results taken at the dimensionless times τ = 0.013, 0.088, 0.168, and 0.245. The vertical temperature stratification is observed. The streamline contours exhibit circulation patterns, which are characterized by the two symmetrical vortices. The fluid flows as it is driven by the effect of buoyancy. This effect is distributed from the top wall of cavity where the fluid is cooled through the partially open surface, causing lower temperature near the top boundary. The existence of the non-uniform temperature along the top surface, and a decrease of density in the direction of gravitational force lead to an unstable condition. Thus the buoyancy effect is associated with the lateral temperature gradients at locations near the top surface. High temperature portions of fluid become lighter than the lower temperature portions at the middle where the wall is open. Theses light portions from two sides then expand laterally towards the center, compressing the lower temperature portions, which are heavier. As a result, the downward flows along the vertical centerline are originated, while the lighter fluid will rise, cooling as it moves. Consequently, the circulation flow pattern is generated. The clockwise and counter-clockwise circulations are located respectively on the left side and right side within the enclosure. The circulations get larger and expand downward with time. An increase in strength of the vortices develops fast during early simulation times, and its maximum magnitude reaches 6.0. Subsequently the vortices are weakened. Similarly, temperature distribution progressively evolves relatively fast in the early times. Slow evolution is observed after that. This result corresponds well with the decrease in strength of flow circulations.

The resulting computational fields of the heating scenario were demonstrated in figure 4. For a purpose of comparison the parameter set remains unchanged. Similarly, the two columns represent temperature and stream function taken at the dimensionless times τ = 0.013, 0.088, and 0.168. The vertical temperature stratification is observed. The streamline contours exhibit circulation patterns, which are characterized by the two symmetrical vortices. The fluid flows as it is driven by the effect of buoyancy. This effect is distributed from the top wall of cavity where the fluid is heated through the partially open area. Unlike the cooling case, in which a presence of negative density mainly causes an unstable condition, in the heating case the lateral density gradient near the top surface is the only cause to the unstable condition that actually leads to the buoyancy force. This reason explains why the heated circulations are weaker than the cooled circulations presented earlier. Heated portions of the fluid become lighter than the rest of fluid, and are expanded laterally away from the center to the sides then flow down along the two vertical walls, leading to the counter-clockwise and clockwise flow circulations. These results suggest that the buoyancy forces are able to overcome the retarding influence of viscous forces. It should be noted that directions of circulations are opposite to those under cooling condition. An increase in strength of the vortices develops fast during early simulation times, and its maximum magnitude reaches 0.25, which is considerably small. Therefore, profiles of temperature contours look similar to those for a stationary fluid, in which the heat transfer is caused by conduction. Similarly, temperature distribution progressively evolves relatively fast in the early times. This result corresponds to the decrease in strength of flow circulations. In the remaining area, the fluid is nearly stagnant suggesting that conduction is dominant due to minimal flow activities. This is because of prevailing viscous effects. It is evident from figures 3 and 4 that the cooling case provides a considerably faster thermal evolution thereby greater convection rate. Furthermore, heat transfer in the vertical direction is much greater than that in the span wise direction. The reader is directed to (Pakdee and Rattanadecho, 2006) for more detailed discussions of heating configuration.

Figure 5 shows the roles of Rayleigh number on heat transfer mechanism. The computed data was extracted at $\tau = 0.155$. Various Rayleigh numbers (Ra = 5×10^3, 10^4, 5×10^4 and 10^5) are examined whereas the Darcy number of 0.1, porosity of 0.8, and h of 60 w/m^2K are fixed. The Rayleigh number provides the ratio of buoyancy forces to change in viscous forces. As Rayleigh number increases, the buoyancy-driven circulations inside the enclosure become stronger as seen from greater magnitudes of stream function. For large Ra (Ra = 5×10^4 and 10^5), contour lines of temperature penetrate faster relative to the low Ra case especially near the central locations. The result is more pronounced for larger Ra. This incident results from strong flow in the downward direction around the central domain. The downward flows assist heat to transfer towards the bottom of the enclosure. In contrast, near the vertical walls where the upward flows are present, the thermal propagation is hindered.

Effects of the Darcy number on the fluid flow and temperature inside the rectangular cavity are depicted in figure 6. The contour of isotherms and streamlines at τ = 0.155 are plotted for different Darcy numbers while ε, Pr and h are kept at 0.8, 1.0 and 60 w/m^2K respectively. Relatively high Ra of 5×10^4 is chosen. The Darcy number, which is directly proportional to the permeability of the porous medium, was set to 0.0001, 0.001 and 0.1. The case in which the porous medium is absent corresponds to infinite Darcy number. The presence of a porous medium within rectangular enclosure results in a force opposite to the flow direction which tends to resist the flow which corresponds to suppress in the thermal currents of the flow as compared to a medium with no porous (infinite Darcy number). It is evident that the increase in Da enhances the streamline intensities thereby assisting downward flow penetration, which causes the streamline lines, i.e., two symmetrical vortices to stretch further away from the top surface. This results in expanding the region for which the convection significantly influences an overall heat transfer process. Further, the evolution results reveal faster rate of vertical temperature distribution than lateral rate. The results are consistent with the thermal behaviors observed in figure 5 for the same reasoning, which confirms how a flow direction impacts the convection heat transfer. On the other hand, as the Darcy number decreases, the flow circulations as well as thermal penetration are progressively retarded due to the reduced permeability of the medium. Figure 6d (Da = 0.0001) indicates that as Darcy number approaches zero, the two circulations confined within the top domain appear very weak. In the remaining area, the fluid is nearly stagnant with very small temperature gradient suggesting that conduction is dominant due to minimal flow activities.

Figure 7 presents how the average Nusselt number changes with time for a variety of Rayleigh numbers. The local Nu at the open portion on the top boundary is computed according to equation (19). The average Nusselt number $\overline{\mathrm{Nu}}$ is then obtained based on equation (20). Initially, the value of $\overline{\mathrm{Nu}}$ decreases rapidly for all cases of Rayleigh numbers, clearly due to the fast reduction of temperature gradients. In the case of low Rayleigh number of $2x10^4$, $\overline{Nu}$ progressively decreases with time. While for higher Ra ($5x10^4$, $8x10^4$), $\overline{Nu}$ values become greater and reach peak values after some time. Further increasing Ra ($8x10^4$), higher maximum Nu is reached more quickly due to greater flow intensities. At late simulation times when stable state is approached, the values of $\overline{Nu}$ continually decrease and essentially level off at late times, thereby diminishing heat transfer by means of heat convection. It can be expected that $\overline{Nu}$ will continue to decrease with time as the steady state is reached.

To gain insights into the observation made, the local values of the corresponding thermal and flow behaviors were traced for Ra of $8x10^4$. The data are extracted and depicted in figure 8 at τ of 0.02, 0.1 and 0.16. The streamlines and isotherms are illustrated in figure 8a-c at τ = 0.02, 0.1 and 0.16 respectively. At τ = 0.02, the averaged Nu is small due to minimal flow activities. Then $\overline{Nu}$ gets higher as the flows gets stronger, which can be seen in figure 8(b) at τ = 0.1. The effect of the rigorous flows overcomes the continual reduction of temperature gradient, resulting in the increase in $\overline{Nu}$. At the subsequent times, the viscous effect increasingly weakens the flows as shown in figure 8(c). As a result, the reduction of temperature gradient prevails, causing $\overline{Nu}$ to decrease. These results correspond well with the variation with time of the averaged Nu, depicted in figure 7. The results confirm the validation of the proposed formulation of Nu.

To better understand the effects of Darcy number on the heat transfer behavior, variations of $\overline{Nu}$ with time for different Darcy number are shown in figure 9. The resulting plots show an interesting evidence of similar variations of $\overline{Nu}$ on Da and those on Ra, which was observed previously in figure 7. Average Nu correlates with Ra in a way similar to correlation of Nu with Da. Further increasing values of Da (0.05 and 0.1) cause larger $\overline{Nu}$ variations.

Locations of the peak values are altered relative to Da value. A peak of profile is reached more quickly for higher Da. Greater Da gives higher $\overline{\mathrm{Nu}}$, suggesting that the higher overall heat transfer rate is due to more energetic vortices. However, $\overline{\mathrm{Nu}}$ substantially reduces at late times.

5. Conclusions

Numerical simulations of natural convection flow through a fluid-saturated porous medium in a rectangular cavity due to cooling convection at top surface were performed. Transient effects of associated controlling parameters were examined. The two-dimensional flow is characterized mainly by two symmetrical eddies that are initiated by the presence of buoyancy effect. In the cooling case, the buoyancy effect is associated not only with the lateral temperature gradient at locations near the top surface, but also with the condition that the density gradient is negative in the direction of gravitational force. On the other hand, the buoyancy force is induced solely by the lateral temperature gradient in the heating case. The cooling and heating flow directions are opposite. Cooling flows are much stronger due to greater buoyancy effects, indicating higher overall convection rate. The heat transfer mechanism is analyzed using the newly derived formulation of Nu. Heat transfer rate is faster around vertical symmetric line relative to the near-wall regions. Large values of Rayleigh number increase streamline intensities, thus enhancing the downward flow penetration. The temperature stratification penetrates deeper toward the bottom wall, and temperature range within the domain is extended. Therefore it enlarges the region where convection mode is significant. Small values of Darcy number hinder the flow circulations. Therefore the heat transfer by convection is considerably suppressed. Furthermore, the new formulation of Nu captures the heat transfer behaviors reasonably correctly. Interestingly, the dependences of Nu on Da and on Ra are found to have the same trends.

Acknowledgments

This research was supported by the Thailand Research Fund (TRF) 2008 under contract number: MRG5180238

References

[1] Al-Amiri, A.M., Analysis of Momentum and Energy Transfer in a Lid-Driven Cavity Filled with a Porous Medium. International Journal of Heat and Mass Transfer, 43, pp.3513-3527, 2000.

[2] Al-Amiri, A.M., Natural convection in porous enclosures: The application of the two-energy equation model, Numerical Heat Transfer Part A, 41, pp.817-834, 2002.

[3] Aydin, O., Determination of Optimum Air-Layer Thickness in Double-Pane Windows. Energy and Buildings, 32, pp.303-308, 2000.

[4] Basak, T., Roy, S., Paul, T., and Pop, I., Natural convection in a square cavity filled with porous medium: Effects of various thermal boundary conditions. International Journal of Heat and Mass Transfer, 49, pp.1430-1441, 2006.

[5] Beckermann, C., Viskanta, R., and Ramadhyani, S., A numerical study of non-Darcian natural convection in a vertical enclosure filled with a porous medium. Numerical Heat Transfer, 10, pp.557-570, 1986.

[6] Bera, P., Eswaran, V., and Singh, P., Numerical study of heat and mass transfer in an anisotropic porous enclosure due to constant heating and cooling. Numerical Heat Transfer Part A, 34, pp.887-905, 1998.

[7] Bera, P. and Khalili, A., Double-diffusive natural convection in an anisotropic porous cavity with opposing buoyancy forces: multi-solutions and oscillations. International Journal of Heat and Mass Transfer, 45, pp.3205-3217, 2002.

[8] Bergman, T.L., Incropera, F.P., and Viskanta, R., Correlation of Mixed Layers Growth in Double-Diffusive, Salt-Stratified System Heated from Below. Journal of Heat Transfer, 108, pp.206-211, 1986.

[9] Bilgen, E. and Mbaye, M., Be'nard cells in fluid-saturated pourous enclosures with lateral cooling. International Journal of Heat and Fluid Flow, 22, pp.561-570, 2001.

[10] Brinkmann, H.C., On the permeability of media consisting of closely packed porous particles. Applied Sciences Research, 1, pp.81-86, 1947.

[11] Bradean, R., Ingham, D.B., Heggs P.J., and Pop, I., The unsteady penetration of free convection flows caused by heating and cooling flat surfaces in porous media. International Journal of Heat and Mass Transfer, 40, pp.665-687, 1997.

[12] Cheng, P., Heat transfer in geothermal systems. Advances in Heat Transfer, 4, pp.1-105, 1978.

[13] Desai, C.P., Vafai, K., and Keyhani, M., On the natural-convection in a cavity with a cooled top wall and multiple protruding heaters, J. Electronic Packaging, 117, pp.34-45, 1995.

[14] El-Refaee, M. M., Elsayed, M.M., Al-Najem, N.M., and Noor, A.A., Natural convection in partially cooled tilted cavities, Int. J. Numerical Methods, 28, pp.477-499, 1998.

[15] Imberger, J. and Hamblin, P.F., Dynamics of Lakes, Reservoirs, and Cooling Ponds. Annual Review of Fluid Mechanics, 14, pp.153-187, 1982.

[16] Khanafer, K.M., Chamkha, A.J., (1998). Mixed Convection Flow in a Lid-Driven Enclosure Filled with a Fluid-Saturated Porous Medium. International Journal of Heat and Mass Transfer 42, 2465-2481.

[17] Khanafer, K. and Vafai, K., Double-Diffusive Mixed Convection in a Lid-Driven Enclosure Filled with a Fluid-Saturated Porous Medium. Numerical Heat Transfer Part A, 42, pp.465-486, 2002.

[18] Kim, S.J., Kim, D., and Lee, D.Y., On the local thermal equilibrium in microchannel heat sinks, Int. J. Heat Mass Transfer, 43, pp.1735-1748, 2000.

[19] Lauriat, G., and Prasad, V., Natural convection in a vertical porous cavity: a numerical study for Brinkmann-extended Darcy formulation. ASME Journal of Heat Transfer, 109, pp.295-320, 1987.

[20] Lauriat, G. and Prasad, V., Non-Darcian effects on natural convection in a vertical porous enclosure. International Journal of Heat and Mass Transfer, 32, pp.2135-2148, 1989.

[21] Marafie, A and Vafai, K., Analysis of non-Darcian effects on temperature differentials in porous media, Int. J. Heat Mass Transfer, 44, pp.4401-4411, 2001.

[22] Mohammad, A.A., Nonequilibrium natural convection in a differentially heated cavity filled with a saturated porous matrix. Journal of Heat Transfer, 122, pp.380-384, 2000.

[23] Nield, D.A., Bejan, A., Convection in Porous Media, Springer, New York, 1999.

[24] Nithiarasu, P., Seetharamu, K.N., and Sundararajan, T., Natural convective heat transfer in a Fluid Saturated variable porosity medium, Int. J. of Heat Mass Transfer, 40, pp.3955-3967, 1997.

[25] Nithiarasu, P., Seetharamu, K.N., and Sundararajan, T., Numerical Investigation of Buoyancy Driven Flow in a Fluid Saturated non-Darcian Porous Medium. International Journal of Heat and Mass Transfer, 42, pp.1205-1215, 1998.

[26] Oosthuizen, P.H. and Patrick, H., Natural Convection in an Inclined Square Enclosure Partly Filled with a Porous Medium and with a Partially Heated Wall, American Society of Mechanical Engineers. Heat Transfer Division, (Publication) HTD 302, pp.29-42, 1995.

[27] Oztop, H.F., Natural convection in partially cooled and inclined porous rectangular enclosure. International Journal of Thermal Sciences, 46, pp.149-156, 2007.

[28] Pakdee, W. and Rattanadecho, P., Unsteady effects on natural convective heat transfer through porous media in cavity due to top surface partial convection Applied Thermal Engineering. 26, pp.2316-2326, 2006.

[29] Pop, I. and Ingham, D.B., Convective Heat Transfer, Mathematical and Computational Modeling of Viscous Fluids and Porous Media, Pergamon, Oxford, 2001.

[30] Ratanadecho, P., Aoki, K., and Akahori, M., A Numerical and Experimental Investigation of the Modeling of Microwave Drying Using a Rectangular Wave Guide. Journal of Drying Technology, 19, pp.2209-2234, 2001.

[31] Ratanadecho, P., Aoki, K., and Akahori, M., Influence of Irradiation Time, Particle Sizes and Initial Moisture Content During Microwave Drying of Multi-Layered Capillary Porous Materials. ASME Journal of Heat Transfer, 124, pp.151-161, 2002.

[32] Wakashima, S. and Saitoh, T.S., Benchmark solutions for natural convection in a cubic cavity using the high-order time-space method, Int. J. Heat Mass Transfer, Vol. 47, pp.853-864, 2004.

[32] Stanish, M.A., Schager, G.S., and Kayihan, F., A., Mathematical Model of Drying for Hygroscopic Porous Media. AIChE Journal, 32, pp.1301-1311, 1986.

[33] Tong, T.W. and Subramanian, E., A boundary-layer analysis for natural convection in vertical porous enclosures-use of the Brinkman-extended Darcy model, ASME Journal of Heat Transfer, 28, pp.563-571, 1985.

[34] Vafai, K., (2000). Handbook of Porous Media, Marcel Dekker, New York.

TABLE

Table 1. Comparison of the results obtained in the present study with those of the benchmark solutions for natural convection of air (Wakashima and Saitoh, 2004).

Ra	ω_{center}	Difference (%)	U_{max}	Difference (%)	V_{max}	Difference (%)
10^4 present	1.111	0.82	0.202	1.51	0.220	0.2
previous work	1.102		0.199		0.222	
10^5 present	0.262	1.55	0.144	1.41	0.249	1.22
previous work	0.258		0.142		0.246	

Table 2. Comparison of the results obtained in the present study with those of Aydin (2000).

	Present work	Published work	Difference (%)
ψ_{max}	5.070	5.087	0.33
U_{max}	16.300	16.225	0.46
V_{max}	19.730	19.645	0.43

Table 3. Comparison of the results obtained in the present study with those of Nithiarasu et al. (1997). (Da=0.01, Ra = 10^4, porosity = 0.6)

	Present work	Published work	Difference (%)
ψ_{max}	2.53	2.56	1.17
V_{max}	9.49	9.34	1.60

LIST of FIGURE CAPTIONS

Figure 1. Schematic representation of the computational domain.

Figure 2. Test results for validation purpose: a) Nithiarasu et al. (1997): Non-Darcian model (including inertial and boundary effect) b) present simulation: Brinkman-extended Darcy model, which accounts for viscous effects.

Figure 3. Sequential files with the cooling boundary for contours of temperature and streamlines at times τ = (a) 0.013, (b) 0.088, (c) 0.168, and (d) 0.245. (Ra = $5\text{x}10^4$, Da = 0.1, Pr =1.0, ε = 0.8, and h = 60 W/m^2K)

Figure 4. Sequential files with the heating boundary for contours of temperature and streamlines at times τ = (a) 0.013, (b) 0.088, and (c) 0.168. (Ra = $5\text{x}10^4$, Da = 0.1, Pr =1.0, ε = 0.8, and h = 60 W/m^2K)

Figure 5. Contours of temperature and streamlines for the cooling case (a) Ra = $5\text{x}10^3$ (b) Ra = 10^4 (c) Ra = $5\text{x}10^4$ (d) Ra = 10^5. (Da = 0.1, h = 60 W/m^2K, Pr = 1.0, and ε = 0.8)

Figure 6. Contours of temperature and streamlines for the cooling case (a) Da = infinity (b) Da = 0.01 (c) Da = 0.001 (d) Da = 0.0001. (Ra = $5\text{x}10^4$, h = 60 W/m^2K, Pr = 1.0, and ε = 0.8)

Figure 7. Variations of the average Nusselt number with time for different Rayleigh numbers. (Da = 0.01, h = 60 W/m^2K, Pr = 1.0, and ε = 0.8)

Figure 8. (a)-(c) temperature contours overlaid by velocity vectors at τ = 0.02, 0.1 and 0.16 respectively. Data is taken from that of figure 7 for Ra = $8\text{x}10^4$.

Figure 9. Variations of the average Nusselt number with time for different Darcy numbers. (Ra = $5\text{x}10^4$, h = 60 W/m^2K, Pr = 1.0, and ε = 0.8)

FIGURES

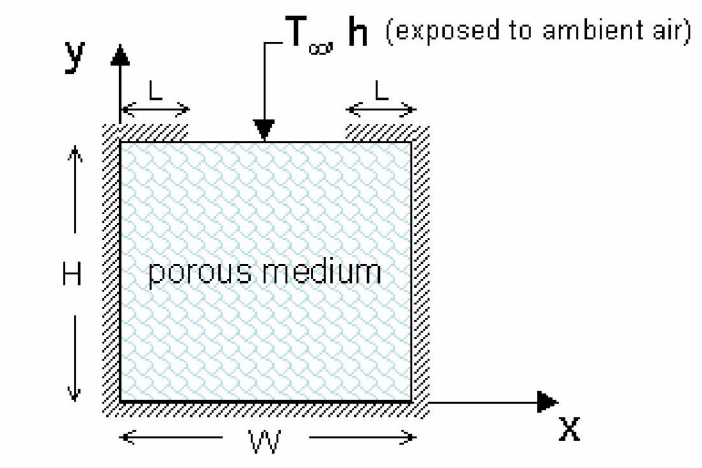

Figure 1

(a)

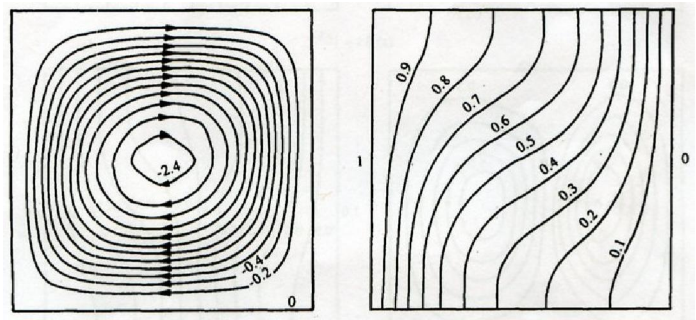

(b)

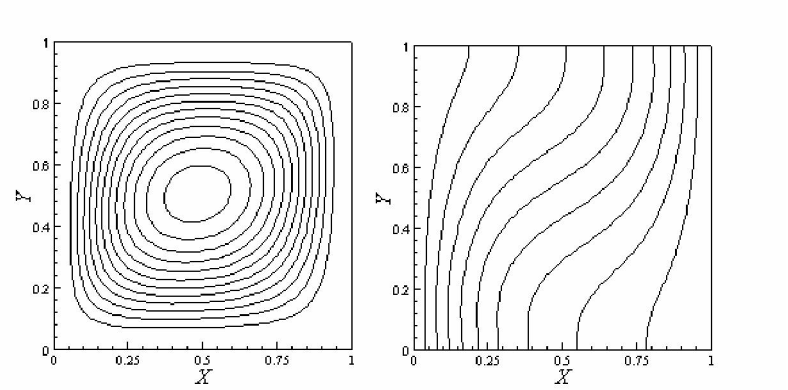

Figure 2

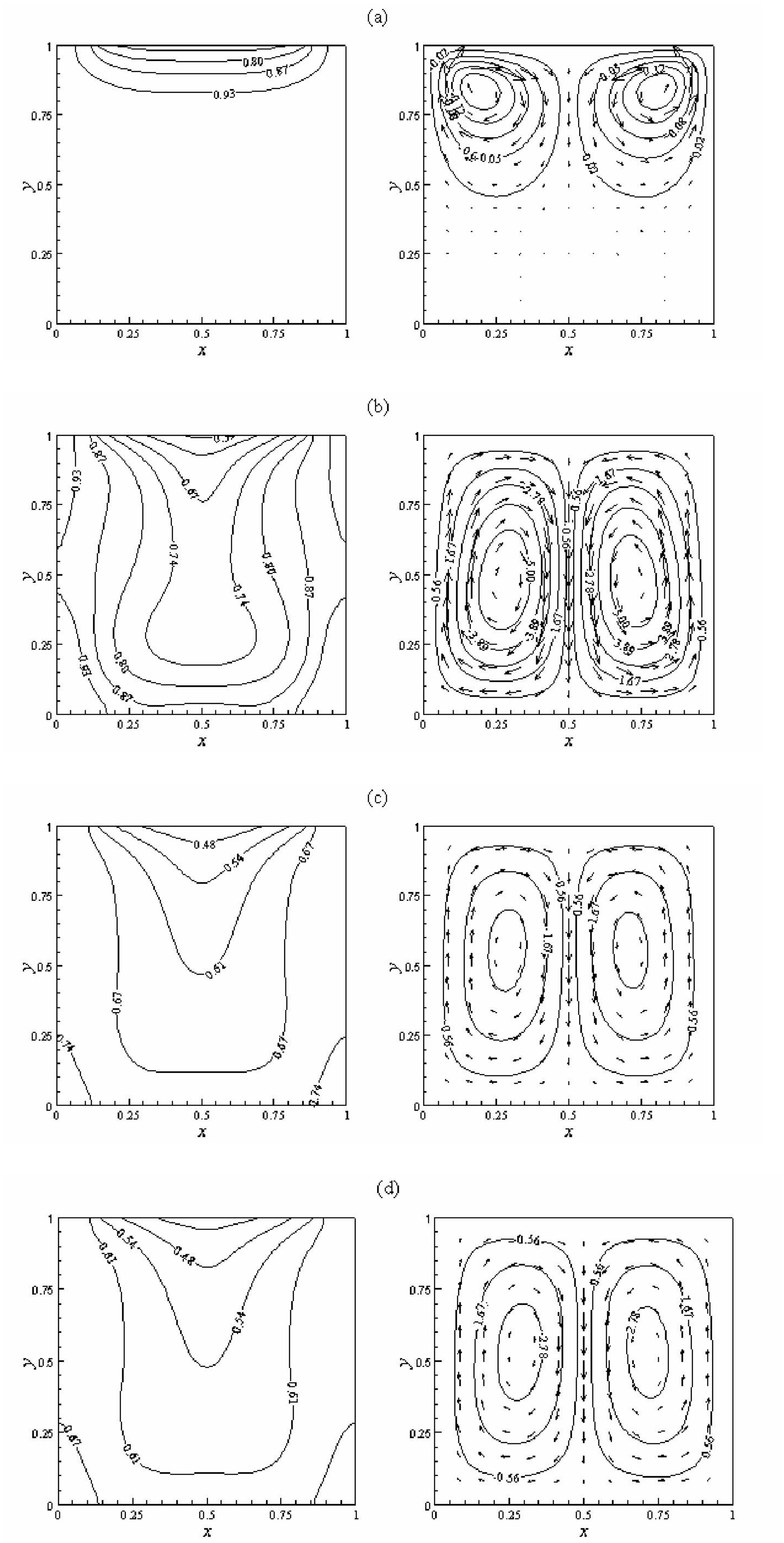

Figure 3

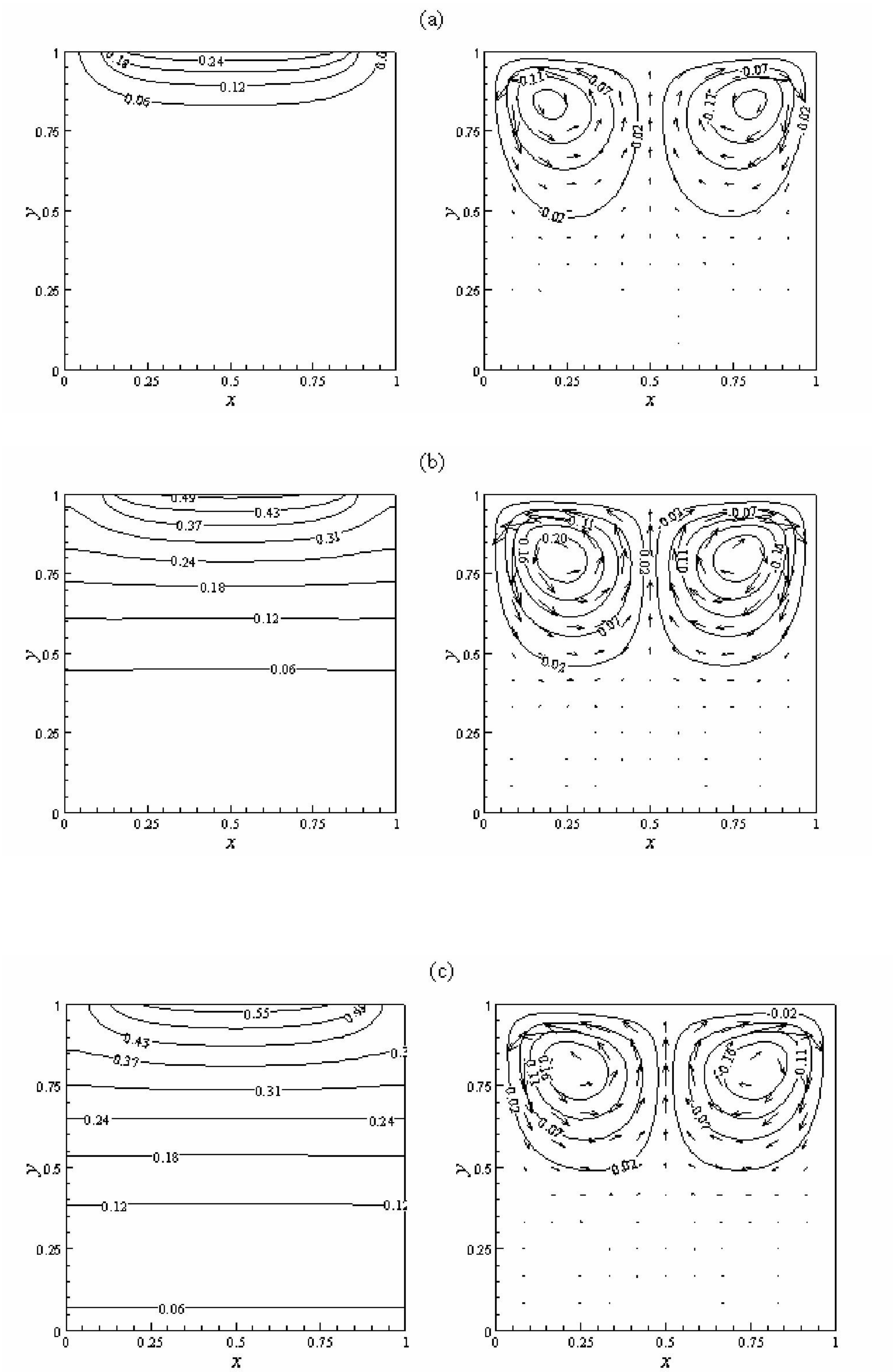

Figure 4

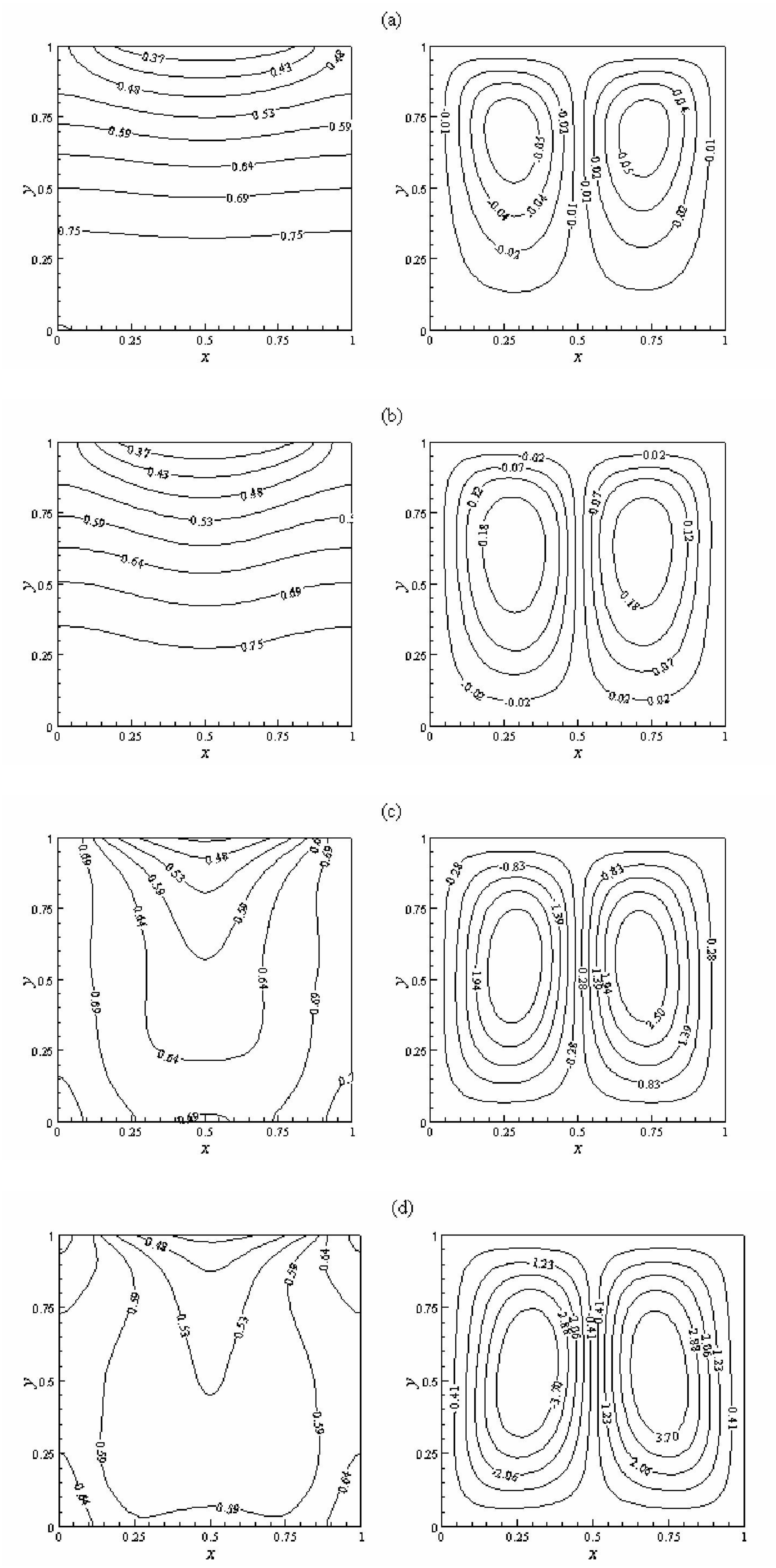

Figure 5

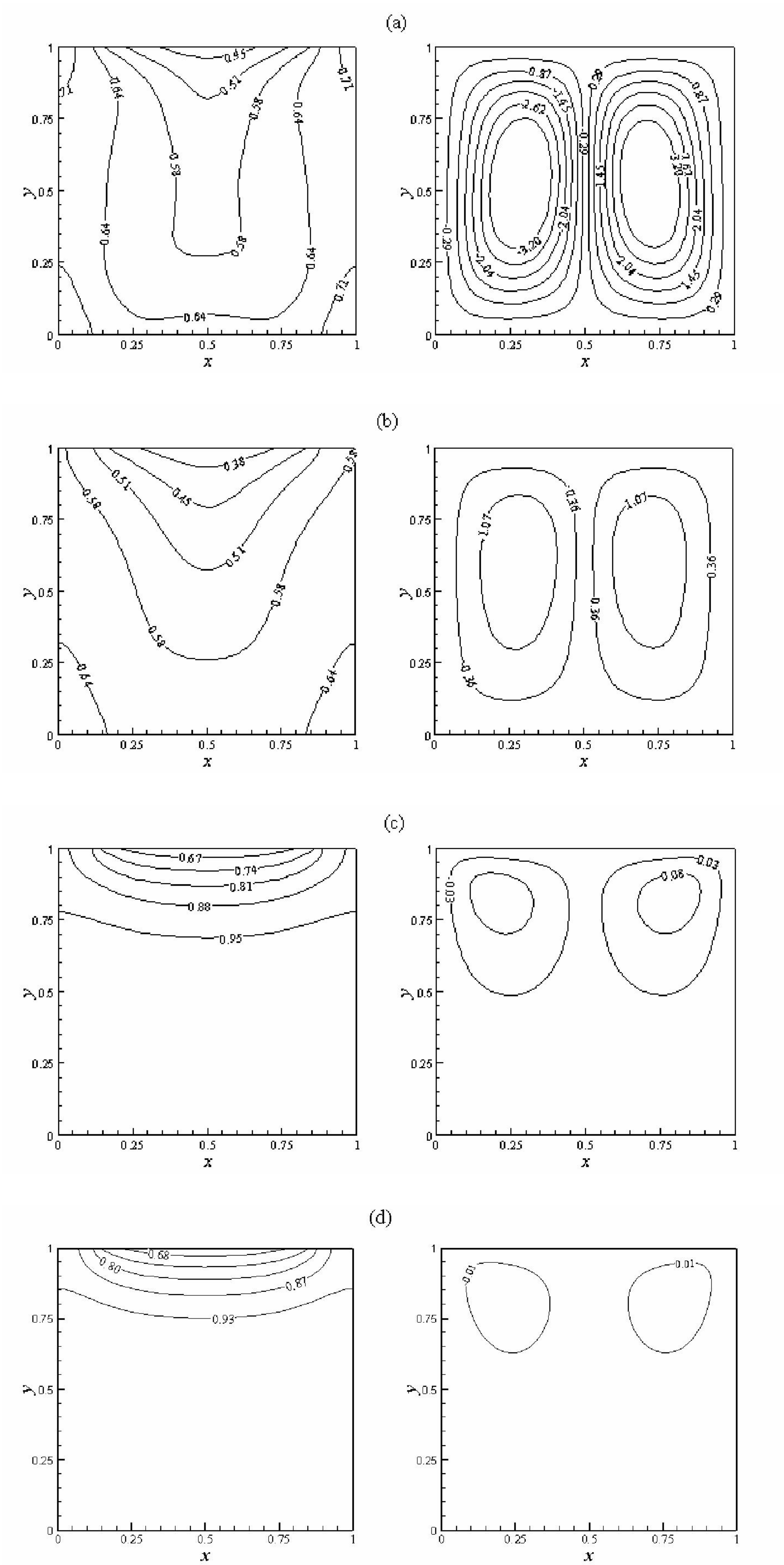

Figure 6

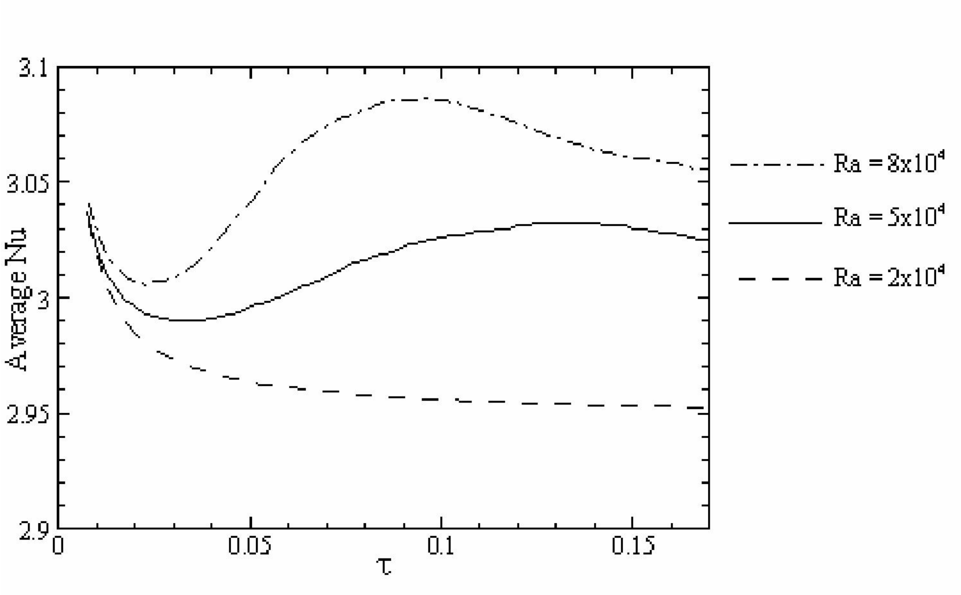
3.1
3.05
3
2.95
2.9
0
0.05
0.1
0.15
τ
Average Nu
Ra = 8x10⁴
Ra = 5x10⁴
Ra = 2x10⁴

Figure 7

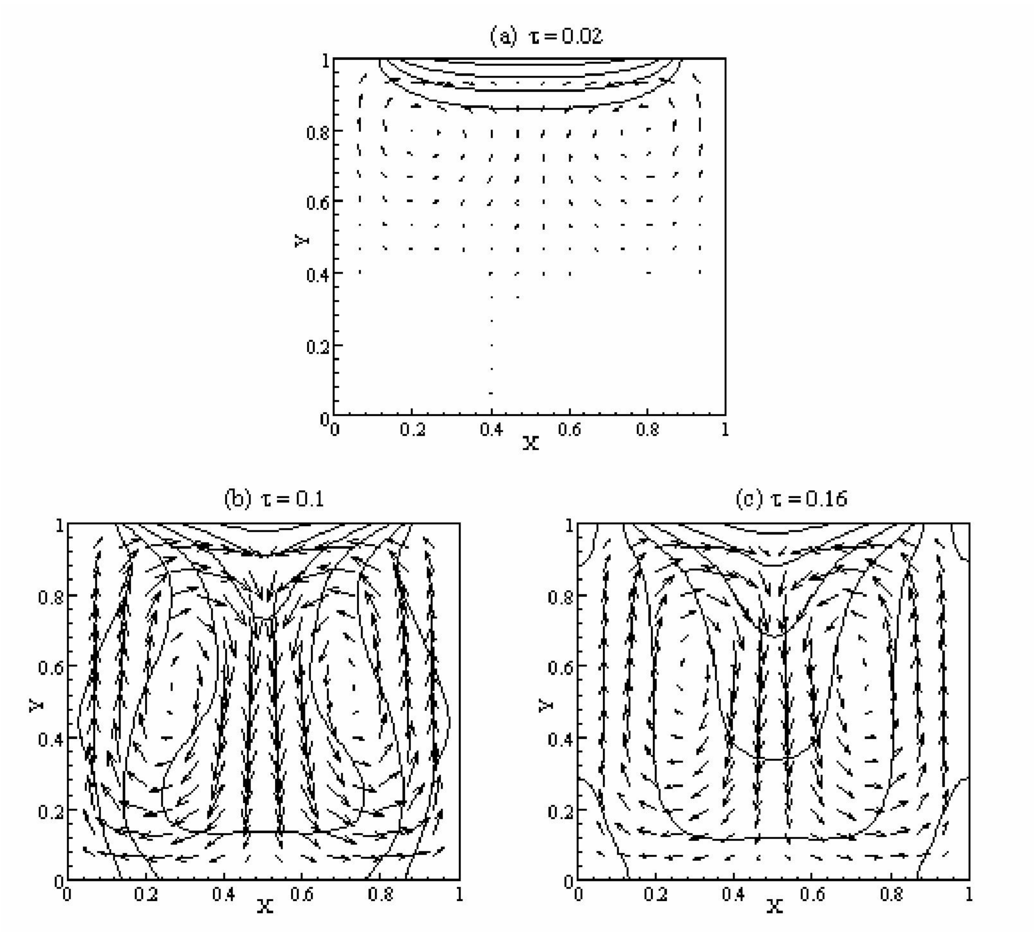

Figure 8

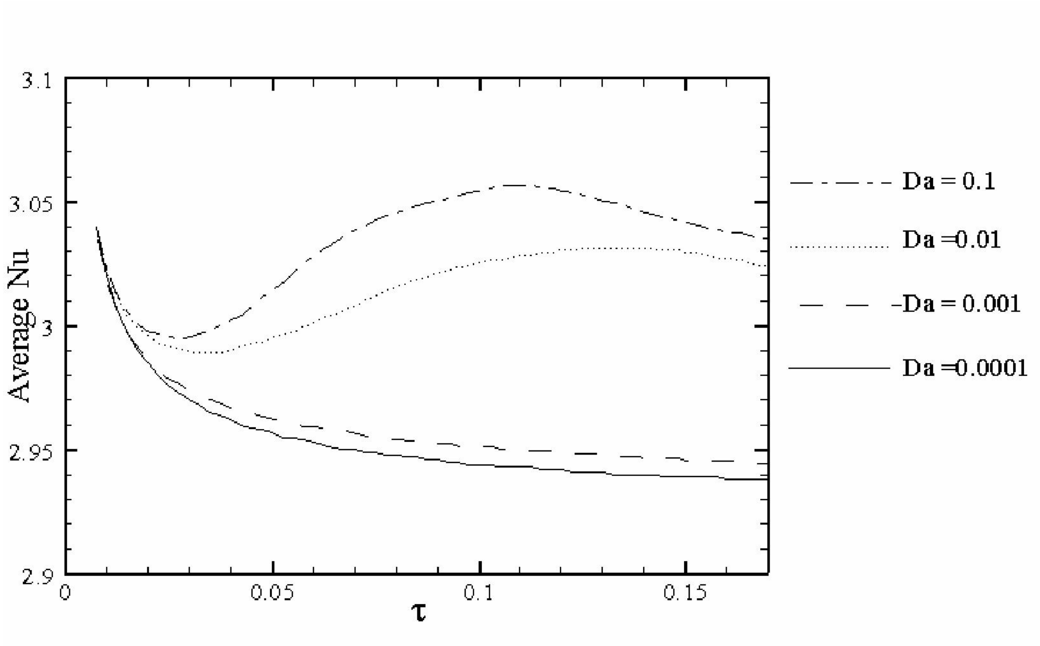
3.1
3.05
3
2.95
2.9
Average Nu
0
0.05
0.1
0.15
τ
Da = 0.1
Da =0.01
Da = 0.001
Da =0.0001

Figure 9